

## INVESTIGATIVE NUCLEAR MEDICINE

Improved Radioimaging and Tumor Localization with Monoclonal  $F(ab')_2$ 

Richard L. Wahl, Charles W. Parker, and Gordon W. Philpott

*Mallinckrodt Institute of Radiology, Howard Hughes Medical Institute at Washington University School of Medicine, and the Jewish Hospital of St. Louis, St. Louis, Missouri*

**Monoclonal anti-tumor antibodies have great promise for radioimmunodetection and localization of tumors. Fab and  $F(ab')_2$  fragments, which lack the Fc fragment of antibody (Ab), are cleared more rapidly from the circulation and may have less nonspecific tissue binding than intact Ab. In radioimaging studies using a murine monoclonal antibody to carcinoembryonic antigen in a human colon carcinoma xenografted into hamsters,  $F(ab')_2$  fragments were shown superior to Fab fragments and intact antibody for scintiscanning. In double-label experiments with anti-CEA antibody and control monoclonal IgG,  $F(ab')_2$  fragments were found to give better and more rapid specific tumor localization than intact antibody or Fab fragments.  $F(ab')_2$  fragments offer significant promise for tumor imaging and possibly therapy.**

**J Nucl Med 24: 316-325, 1983**

Although polyclonal antibodies have shown promise for the localization and radioimmunodetection of malignancies (1-3), the development of monoclonal antibodies has heightened interest in this approach to tumor detection (4-6). Although intact antibody is cleared relatively rapidly from the bloodstream significant background radioactivity remains for several days after injection (7-10). This has made computer-aided background subtraction of a second nonspecific (blood-pool) radioagent helpful to image the tumor within 2 days of injection. Although extremely helpful when conducted by those expert in the technique, this type of imaging exposes the patient to additional radiation and adds several potential sources of error (3,4,11,12). Antibodies of high specificity that are cleared more rapidly from the circulation are thus desirable, and the elimination of the Fc portion of antibodies is of potential benefit in that regard (13). Limited work to date has been inconclusive but encouraging, particularly in terms of better access of  $F(ab')_2$  to the central nervous system, but monoclonal antibody frag-

ments have not been extensively studied (6,14-17). Recent work with polyclonal affinity-purified anti-CEA, however, has suggested that intact antibodies are localized by the tumor better than fragments (18). In this report we compare the behavior of intact I-131 labeled murine monoclonal anti-carcinoembryonic antigen (CEA) and its Fab and  $F(ab')_2$  fragments, as well as an I-131 labeled nonspecific control IgG and its fragments in imaging a human colon cancer (GW-39) xenografted into hamsters (19). Double-label experiments using I-131 anti-CEA and I-125 monoclonal IgG without known affinity were also performed to evaluate specificity.

## METHODS

The preparation of our IgG<sub>1</sub>, kappa monoclonal antibody to CEA, has been partially described (20). Briefly, CEA was extracted from the human colon cancer GW-39 to hyperimmunize BALB/c mice. Splenocytes were fused with NS-1 mouse myeloma cells using a method adapted from Galfré et al (21). A positive clone was selected by radioimmunoassay\* isolated by limiting dilution, and grown intraperitoneally in pristane-primed BALB/c mice. Antibody was purified

Received July 19, 1982; revision accepted Dec. 20, 1982.

For reprints contact: Dr. Richard L. Wahl, Div. of Nucl. Med. Mallinckrodt Institute of Radiology, 510 South Kingshighway, St. Louis, MO 63110.

from the ascitic fluid by  $(\text{NH}_4)_2\text{SO}_4$  fractionation and Sephadex G-200 chromatography. Radioiodination was performed using a lactoperoxidase method previously described using carrier-free I-131 or I-125 (22). Immunoreactivity was determined using CEA (extracted from GW-39 tumors) immobilized on Sepharose beads by guinea pig anti-CEA antibody.<sup>†</sup> Exhaustive absorption of intact I-125 anti-CEA with this solid phase CEA (3 absorptions for 18 hr at 37°C) showed a total binding of greater than 70% of this preparation. Control binding studies using I-125 anti-CEA and beads without CEA or I-125 MOPC21 IgG and beads coated with CEA showed binding of less than 5% to 18%. Titration and saturation analysis, using the radioimmunoassay\* adapted kit with the CEA provided in this kit as antigen, showed the avidity of the anti-CEA for this CEA to be greater than  $1 \times 10^9$  moles<sup>-1</sup>. The specificity for CEA was confirmed by in vitro cell-binding assays in which up to 59% of antibody protein bound to CEA-producing human colon cancer cells but only 0.1% to 17% bound maximally to other non-CEA-producing human cells, including human granulocytes and lymphocytes, or normal hamster liver cells (unpublished results). By contrast, a control monoclonal IgG<sub>1</sub> kappa from MOPC21 murine myeloma, without known specificity, showed less than 6% binding to CEA-producing target cells.

Fab fragments were prepared using 2% papain by a modification of the method of Porter (23).  $\text{F(ab')}_2$  fragments were prepared using a modification of the method of Nisonoff et al (24; Nisonoff, A., personal communication). 2.5% pepsin was added to intact antibody in 0.2 N sodium acetate buffer, pH 4.2, and incubated at 37°C for 24 hr. The purity of intact antibody and fragments was confirmed by 7.5% SDS-PAGE analysis in unreduced gels (25). Pepsin and papain were removed by dialysis. Undigested IgG was removed by chromatography with Sephadex G-100 for Fab or G-200 for  $\text{F(ab')}_2$ . Antibody and fragment concentrations were quantitated by absorbancy at 280 nm ( $E_{280}^{1\%} = 14$ ). The binding of the IgG fragments to immobilized CEA and CEA-producing and -nonproducing cells was comparable to that of the intact antibody. In an abbreviated assay (one absorption for 2 hr at 45°C) with CEA extracted from GW-39 immobilized on Sepharose beads (Abbott kit), bindings of radioiodinated intact anti-CEA,  $\text{F(ab')}_2$ , and Fab were 27%, 26%, and 22%, respectively, whereas binding to beads without CEA was 1% to 4%. Binding of control MOPC IgG, intact and fragments, in this assay using beads with CEA ranged from 0.1 to 2% of cpm added. Maximal bindings to freshly isolated, mechanically dispersed GW-39 cells in vitro by intact anti-CEA,  $\text{F(ab')}_2$ , and Fab were 56%, 51%, and 62%, whereas binding by intact MOPC IgG and fragments was 4% to 6%. Bindings of intact anti-CEA, MOPC IgG, and their fragments to normal hamster liver cells and to

non-CEA-producing target cells (HeLa) ranged from 0.5% to 14%. Preliminary studies have shown little or no binding of I-125-anti-CEA to human lymphocytes or granulocytes *in vitro*.

For radioimaging, 16 hamsters bearing GW-39 tumors of about 5 g in the right thigh muscle were injected intracardially with 40–50  $\mu\text{Ci}$  (approximately 10–20  $\mu\text{g}$ ) of I-131-labeled anti-CEA antibody or active fragments in phosphate-buffered saline containing 10% normal hamster serum (v/v). Drinking water contained Lugol's iodide for 10 days before and during the study. Images were obtained using a gamma camera with a 4 mm high-energy pinhole collimator. Ten to twenty thousand counts were recorded on Polaroid film. Animals were sedated for imaging with 5 mg of intraperitoneal pentobarbital.

An additional 26 animals bearing approximately 1 g tumors were studied in a similar fashion. These animals received 50  $\mu\text{Ci}$  (10–20  $\mu\text{g}$ ) of I-131-anti-CEA intact or its fragments or 50  $\mu\text{Ci}$  of I-131-MOPC or its fragments. Images were obtained as previously and also collected on a digital computer with a  $64 \times 64 \times 8$  matrix, which could accomplish uniform background subtraction.

Double-label experiments (26) using simultaneous injections of I-131-anti-CEA and I-125 MOPC IgG were performed to evaluate the specificity of antibody localization in the tumor (Table 1). Radioiodinated fragments or intact IgG were injected into 68 animals with small tumors (generally less than 1 g) in the right thigh; blood, tumor, and tissues were assayed 6 hr, 1, 2, 3, 5, or 7 days later. Organs were weighed and then counted in a gamma counter. After correction for physical decay rates and downscatter of I-131, the percentage of injected dose bound per g of tissue, and the tissue-to-blood ratios were calculated. Tumor-to-nontumor ratios were calculated from the cpm/g of tumor divided by cpm/g of tissue. Localization ratios were calculated from the tumor-to-nontumor ratios for anti-CEA divided by the tumor-to-nontumor ratios for MOPC21.

## RESULTS

Scintiphotos obtained at 2, 6, and 11 days after injection of intact I-131 anti-CEA (Fig. 1) showed that although the tumor was visible at 2 days, it took 6–11 days for background radioactivity to decrease so that the tumor was well defined (8). The images in Fig. 1B, C, D are representative of the four animals studied.

One and two days after injection of I-131 Fab fragments, the scans of the seven animals with larger tumors demonstrated significant radioactivity in the abdomen, primarily in the liver, stomach, kidneys, and bladder (Fig. 2A, B). There was some radioactivity in the tumor as well, but it was not well delineated. At 3 days after

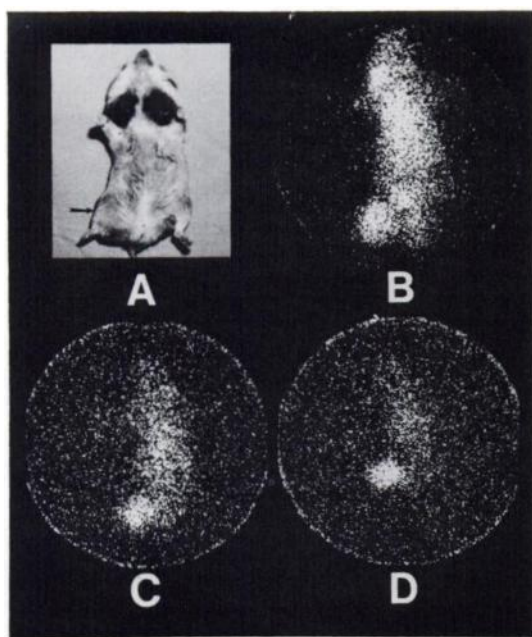


**FIG. 1** (A) Golden Syrian hamster with a 4-to-5 g GW-39 tumor implanted in right thigh (arrow). All scintiphotos were taken in supine position with 4 mm high energy pinhole collimator using 5 mg pentobarbital intraperitoneally for anesthesia. All drinking water contained Lugol's iodide for 10 days previous to and during study. Images were obtained at 24-hr intervals and 15K to 20K counts were recorded per image on Polaroid film. (B) Scintiphoto taken at 2 days after injection of intact I-131 anti-CEA. Image shows white outline of hamster with tumor seen in right proximal thigh. Bladder is seen just medial to tumor. (C) At 6 days slightly less magnified image shows tumor in right thigh region of same animal. Entire animal is still outlined consistent with residual radioactivity in blood pool. (D) At 11 days still slightly less magnified image shows tumor in same animal and further decrease in nonspecific blood pool radioactivity. At sacrifice this tumor weighed ~ 10 g.

injection very little radioactivity remained in these animals (Fig. 2C). Most of the radioactivity (I-131) recovered from the gastric contents was dialyzable, suggesting that *in vivo* deiodination of protein might partly be responsible for the rapid clearance of Fab. The injection mixture did not contain significant I-131 not bound to protein. The litter of these animals was heavily contaminated with I-131, however, and ingestion of free I-131 probably contributed to the stomach and bladder radioactivity. In later experiments in animals with smaller tumors, more frequent litter changes seemed to lessen stomach I-131 radioactivity.

Images obtained with F(ab')<sub>2</sub> fragments at 2 days after injection showed clear definition of the tumor, with some background radioactivity (Fig. 3A). This image is comparable to the 6-day intact antibody image (Fig. 1C). At 3 days after injection (Fig. 3B) background radioactivity was decreased and the image was not significantly different from that of intact antibody at 11 days (Fig. 1D). By 4 days the hamster body was barely visible, and only the tumor was clearly seen (Fig. 3C). Later images at 7 days showed little or no radioactivity

remaining in the animals. Results were similar for the five animals with relatively large tumors imaged in this fashion.

Since these tumors can accumulate IgG nonspecifically (10), we also studied 26 animals injected with MOPC IgG as well as with anti-CEA, intact and fragments, labeled with I-131. At the time of injection, the hamsters weighed 120–140 g and the implanted tumors about 1.2 g. The animals received 50  $\mu$ Ci of Ab or fragments (10 to 20  $\mu$ g). The results were similar to those in animals with larger tumors though the small tumor size seemed to be approaching the limits of detection at this dose without background subtraction. At 2 days following injection anti-CEA F(ab')<sub>2</sub> fragments showed clearer definition of tumors as compared with MOPC F(ab')<sub>2</sub> fragments (Fig. 4C, D). Radioactivity in the bladder and stomach was largely due to consumption of I-131 laden litter. Frequent litter changes greatly reduced this radioactivity in the stomach and bladder without affecting tumor localization, and improved the tumor imaging with the F(ab')<sub>2</sub> fragment of anti-CEA but not with MOPC.

Computer subtraction of a uniform level of background radioactivity provided more clearly defined tumor images at earlier time points with anti-CEA F(ab')<sub>2</sub>. With this technique it was possible to enhance the tumor definition relative to the normal tissues with anti-CEA F(ab')<sub>2</sub> by 2 days after injection. Increased

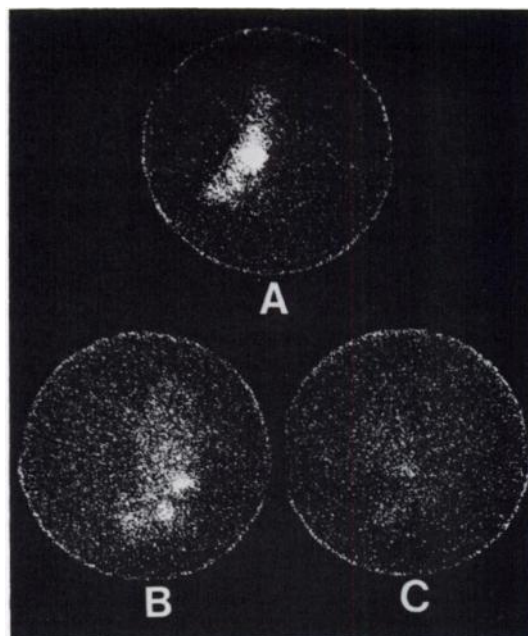


**FIG. 2** (A) Image of hamster injected 1 day previously with 50  $\mu$ Ci of I-131 anti-CEA Fab fragments. Radioactivity in upper abdomen is due largely to gastric contents and kidneys. Tumor is seen in right thigh. (B) At 2 days abdominal I-131 has decreased, though left upper abdominal radioactivity is still seen. Midline radioactivity in lower abdomen is the bladder. Urinary catheterization removed much of this radioactivity. Tumor is seen faintly in right leg. (C) Image at 3 days. Almost no radioactivity remains in this animal.

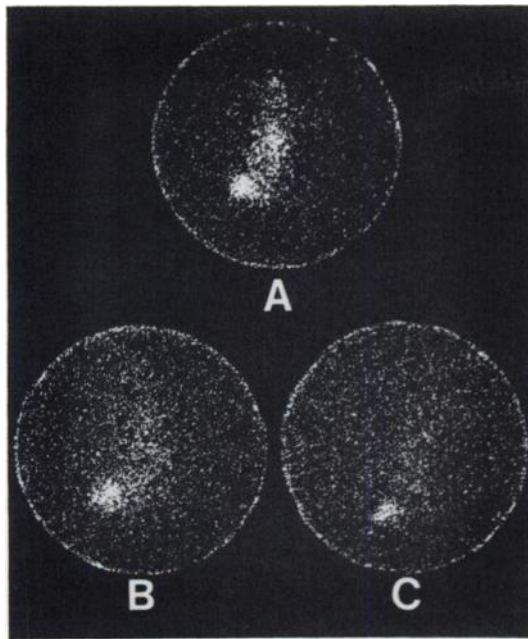


**FIG. 3** (A)  $F(ab')_2$  image at 2 days after injection of 44  $\mu\text{Ci}$  of  $^{131}\text{I}$ -anti-CEA  $F(ab')_2$  shows tumor uptake and is comparable to 6-day intact-antibody image (Fig. 1C). (B) Image at 3 days shows decrease in blood-pool radioactivity seen at 2 days; this image is quite similar to 11-day intact-antibody image, allowing for slightly smaller tumor size in this animal (9 g compared with 11 g) and slightly smaller injected dose (44 compared with 50  $\mu\text{Ci}$ ). (C) At 4 days only tumor radioactivity is seen, without hamster body background. Absolute intensity of tumor has decreased more than 9% physical decay expected. By 6–7 days almost no radioactivity was seen in animal or tumor.

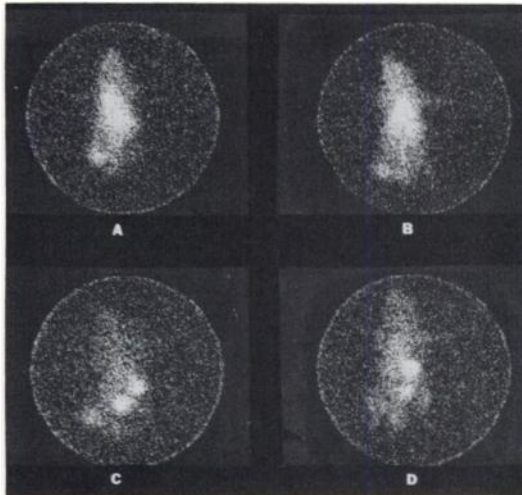


**FIG. 4** (A) Image taken 2 days after injection 50  $\mu\text{Ci}$  anti-CEA intact IgG in animal with approximately 1 g tumor. (B) Image at 2 days after injection MOPC intact IgG in similar animal. Note little difference from anti-CEA intact. (C) Image at 2 days after injection of anti-CEA  $F(ab')_2$ . Tumor appears to be whiter than background (animal consumed  $^{131}\text{I}$ -laden bedding yielding radioactivity in bladder and stomach). One g tumor size is near limit of our technique's sensitivity. (D) Image at 2 days after injection MOPC  $F(ab')_2$  shows poor tumor definition.

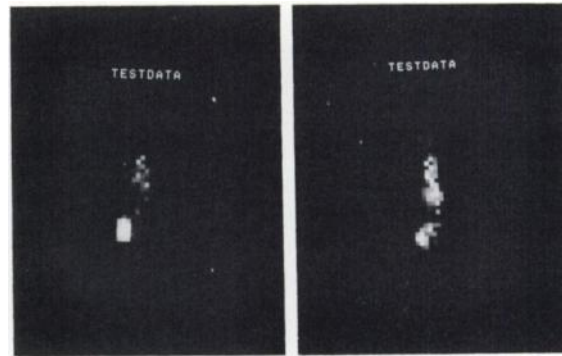


**FIG. 5.** Images obtained by computer subtraction of background 2 days after injection of 64  $\mu\text{Ci}$  into hamsters with 2.5 g tumors in right thigh. (Left) anti-CEA  $F(ab')_2$ . Note large intense white area representing tumor. (Right) MOPC21  $F(ab')_2$ . Note less tumor accretion and increased activity in chest and abdomen.

doses (64  $\mu\text{Ci}$ ) in slightly larger tumors demonstrated the tumor definition quite well (Fig. 5, left). The MOPC  $F(ab')_2$  showed much less tumor uptake and more accretion in the liver (Fig. 5, right). Unprocessed images also showed these differences, but this simple background subtraction technique improved tumor definition.

Images without subtraction using intact anti-CEA or MOPC looked nearly identical at 2 days after injection because of high background levels (Fig. 4A, B). Simple background subtraction techniques provided well-defined tumor images with intact anti-CEA by 6 days after injection (Fig. 6, left), whereas intact MOPC yielded very little concentration of activity in the tumor and still showed significant accumulation in the liver (Fig. 6, right). Images at earlier time points (3½ to 4 days) also showed this difference but were not as striking and clearly inferior to the  $F(ab')_2$  anti-CEA at 2 days.

Imaging with Fab fragments was not satisfactory: imaging was tried before 24 hr and this was not satisfactory either. The tumor was visualized but so was the rest of the animal, especially the kidneys.

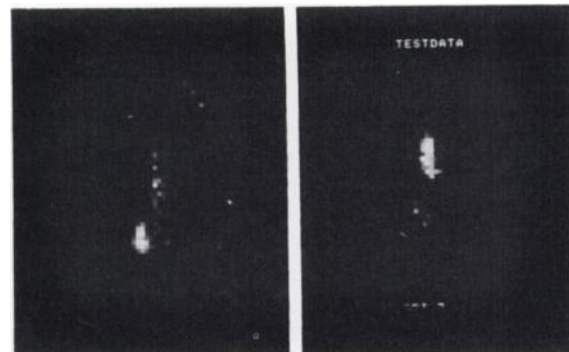


**FIG. 6.** Images obtained by computer subtraction of background 6 days after injection of 50  $\mu\text{Ci}$  into hamsters with 1.2 g tumors into right thigh. (Left) intact anti-CEA. Note tumor in right thigh. (Right) intact MOPC. There is little tumor radioactivity but much remains in chest and abdomen.



The double-label experiments demonstrated that, as expected, antibody fragments without the Fc portion were cleared more rapidly from the circulation than intact anti-CEA and MOPC IgG (Table 1). The Fab fragments, however, were cleared the most rapidly, in contrast to the findings in some studies with other species (7). Lower molecular weight and univalency of I-131 Fab and rapid *in vivo* deiodination may have contributed to this clearance. By 2 days after injection, most of the Fab fragment radioactivity had been excreted and the total tumor accretion was extremely low (0.1% of injected dose per g for anti-CEA Fab, compared with 2.6% per g for intact anti-CEA and 1.1% per g for anti-CEA F(ab')<sub>2</sub>).

In blood clearance rate, F(ab')<sub>2</sub> was intermediate between those of intact Ab and Fab. At one day after injection blood levels of anti-CEA F(ab')<sub>2</sub> were about half the level of intact Ab in blood and by 2 days the level had dropped to less than one fourth. At 2 days the Fab blood level was less than one fifth of the F(ab')<sub>2</sub> blood level and quickly dropped to a nearly unmeasurable range by 3 days after injection (Table 1). For both MOPC and anti-CEA, Fab was cleared significantly faster than F(ab')<sub>2</sub>, which was cleared faster than intact Ab.

Blood levels for intact and F(ab')<sub>2</sub> anti-CEA appeared slightly lower than for MOPC but were different ( $p < 0.01$ ) only at day 5 for intact and day 1 for F(ab')<sub>2</sub>. Fab blood levels for anti-CEA and MOPC were not significantly different except at later times when values were too low to be meaningful.

The antibody fragments and intact antibody behaved differently *in vivo* in terms of tissue binding (Figs. 7–9). The intact anti-CEA had a higher tumor-to-blood ratio than intact MOPC, and it increased gradually, reaching a peak at about 5 days after injection (Fig. 7). There was some nonspecific tumor uptake of intact MOPC IgG, but accretion was less than with intact anti-CEA ( $p < 0.0001$ ). The maximal tumor-to-blood level for intact anti-CEA (1.91) was reached on day 5, with lower tis-

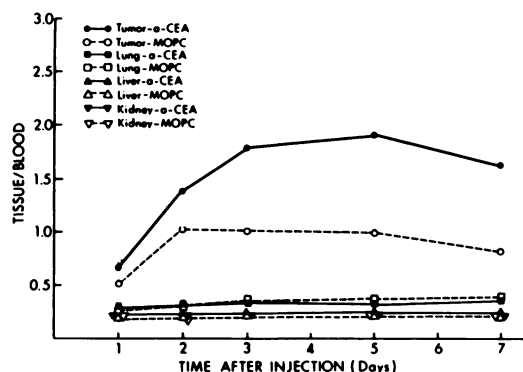


FIG. 7. Intact IgG cpm/g tissue/Intact IgG cpm/g blood vs. time post-injection. Note gradual separation between specific and non-specific IgG in the tumor. (S.E.M.'s are similar to those in Fig. 9 but not shown due to Journal policy).

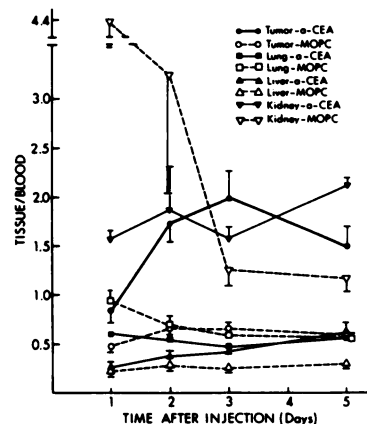


FIG. 8. Fab IgG cpm/g tissue/Fab IgG cpm/g blood  $\pm$  SEM vs. time after injection. Note relatively rapid rise in tissue-to-blood levels. Note striking elevation of both MOPC and anti-CEA kidney radioactivity compared with tumor and blood.

sue-to-blood ratios for intact anti-CEA seen for all other tissues at all time points ( $p < 0.0001$ ) (Fig. 7).

Fab fragments of anti-CEA also had tumor-to-blood ratios approaching two by 3 days after injection (Fig. 8), whereas the mean ratios for MOPC Fab were significantly less ( $p < 0.0001$ ). Early in the time period studied, relatively high levels of nonspecific Fab radioactivity were seen in the kidney, with tissue-to-blood ratios over four for MOPC at 1 day and remaining well above tumor-to-blood levels for MOPC Fab throughout the 5 days. Relatively high levels of anti-CEA Fab were also seen in the kidney throughout the study—as contrasted with experiments involving the intact antibody or F(ab')<sub>2</sub> fragments. Anti-CEA Fab binding to other normal tissues was lower, with tissue-to-blood ratios less than one, but ratios tended to be slightly higher than with intact Ab. We note that Fab blood levels at 3 days were less than 3% of intact Ab levels (Table 1).

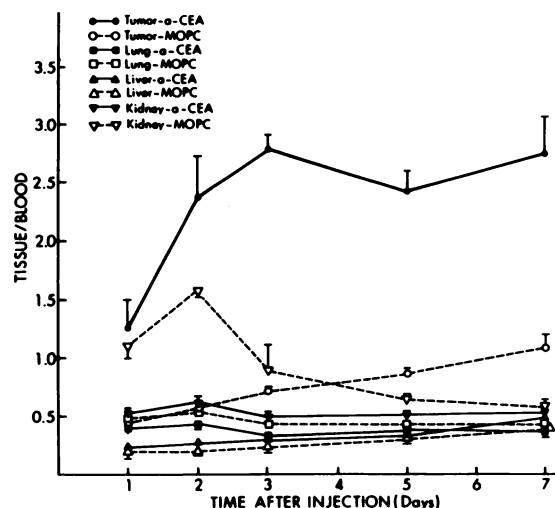


FIG. 9. F(ab')<sub>2</sub> cpm/g tissue/F(ab')<sub>2</sub> cpm/g blood vs. time. Note development of high tissue-to-blood levels early without elevation of anti-CEA kidney radioactivity. Note especially at 1–2 days higher level of F(ab')<sub>2</sub> anti-CEA in tumor compared with all other organs.

TABLE 1. BLOOD LEVELS: INTACT ANTI-CEA AND MOPC IgG AND THEIR FRAGMENTS

Day	Mean percent injected dose per gram blood $\pm$ s.e.m. or range			
	1	2	3	5
Intact*	3 <sup>†</sup>	3	4	4
a-CEA	2.94 (2.5–3.61)	1.87 (1.71–1.98)	1.26 (0.86–1.63)	0.77 (0.70–0.91)
MOPC	3.09 (2.69–3.68)	2.11 (1.92–2.23)	1.46 (0.98–1.81)	0.99 (0.94–1.12)
F(ab') <sub>2</sub>	3	4	4	4
a-CEA	1.37 (1.14–1.51)	0.44 (0.42–0.46)	0.27 (0.25–0.29)	0.13 (0.10–0.15)
MOPC	2.09 (1.74–2.34)	0.60 (0.57–0.64)	0.28 (0.24–0.33)	0.08 (0.07–0.09)
Fab <sup>‡</sup>	8	6	6	8
a-CEA	0.31 $\pm$ 0.10	0.08 $\pm$ 0.01	0.04 $\pm$ 0.002	0.01 $\pm$ 0.001
MOPC	0.32 $\pm$ 0.12	0.08 $\pm$ 0.01	0.02 $\pm$ 0.003	0.02 $\pm$ 0.002

\* Blood levels of intact anti-CEA and MOPC are greater than those of F(ab')<sub>2</sub>, which are greater than those of Fab ( $p \leq 0.01$ ).

<sup>†</sup> Number of animals: Sixty-two hamsters with about 1-gram tumors in the right thigh were injected with 3  $\mu$ Ci I-131a-CEA (1–2  $\mu$ g) and 3  $\mu$ Ci I-125MOPC (1–2  $\mu$ g), intact IgG or fragments. Blood cpm/g were measured and percent injected dose/g calculated correcting for physical decay and downscatter. Each value is mean  $\pm$  s.e.m. or range for 3–8 animals.

<sup>‡</sup> At 6 hr Fab anti-CEA had 0.82  $\pm$  0.17% and MOPC Fab 1.03  $\pm$  0.21% of injected dose/g blood.

Due to their fast clearance, Fab fragment distributions were also measured at 6 hr after injection. Only 0.3% of the injected anti-CEA dose and 0.28% of MOPC Fab remained in the tumor. The anti-CEA tumor-to-blood ratio was 0.38% and the tumor-to-kidney ratio was only 0.12% for four animals studied. The tumor-to-liver ratio for anti-CEA Fab at 6 hr after injection was 1.73 compared with 1.42 for MOPC IgG. All of these ratios suggest images without background subtraction would be suboptimal at this early time point due to high blood pool radioactivity. Images at 20 hr after injection of anti-CEA Fab were no better than those obtained at 1 day (Fig. 2A).

In contrast to Fab fragments and intact Ab, anti-CEA F(ab')<sub>2</sub> attained higher tumor-to-blood ratios (Fig. 9) and did so more promptly than intact Ab (2.38 at 2 days after injection as compared with 1.39 for intact antibody and 1.73 for Fab). This ratio for F(ab')<sub>2</sub> increased to 2.8 at 3 days compared with 1.79 for intact Ab and 2.0 for Fab. Tumor-to-blood ratios for F(ab')<sub>2</sub> of anti-CEA were significantly different at all time points from both intact antibody and Fab ( $p < 0.0001$  by regression analysis), but Fab and intact antibody were not different. Also of note is the fact that the anti-CEA radioactivity in the kidney with F(ab')<sub>2</sub> was about as low as in other nontumor tissues, in marked contrast to the Fab behavior (the level of anti-CEA Fab in the kidney was about equal to that in the tumor). The large difference between anti-CEA F(ab')<sub>2</sub> in the tumor compared with MOPC F(ab')<sub>2</sub> in the tumor at 2 to 3 days should be noted—in contradistinction to the intact Ab data.

Tumor-to-tissue (nontumor) ratios showed that by 3 to 5 days, intact anti-CEA levels were significantly higher in the tumor than intact MOPC relative to normal tissues (Table 2). The higher tumor-to-nontumor ratios for anti-CEA were a result of the specific component of

the antibody binding. The earlier achievement of significant differences between anti-CEA and MOPC fragments by days 1–2 after injection shows retention of the specific component of anti-CEA binding with a relatively rapid reduction in nonspecific binding.

Anti-CEA F(ab')<sub>2</sub> also developed a higher tumor-to-liver ratio at day 1 than did Fab or intact Ab. The anti-CEA F(ab')<sub>2</sub> tumor-to-lung and tumor-to-spleen ratios were also higher on day 3 than were those of intact antibody or Fab (Table 2). There were also trends toward F(ab')<sub>2</sub> tumor-to-tissue ratios being higher than those of intact Ab in the spleen and lung, at all time points. With the number of animals used, these trends were not statistically significant (see Table 2).

The representative specific localization ratios (Table 3) clearly show the superiority of anti-CEA over MOPC for tumor localization in this study. More importantly, they support the conclusion that at least early after injection, F(ab')<sub>2</sub> fragments have a higher specific localizing capability than intact antibody, and probably than Fab fragments. Statistical analyses consistently showed specific F(ab')<sub>2</sub> localization to be significantly higher than intact Ab and sometimes higher than Fab. Except for liver and kidney, however, F(ab')<sub>2</sub> and Fab differences were not statistically different in this small sample size. The total accretion of Fab in the tumor was, of course, much less than with F(ab')<sub>2</sub>.

#### DISCUSSION

The scintigrams obtained using intact antibody without background subtraction provide adequate tumor delineation, but a significant delay exists before there is adequate clearance of the background radioactivity to allow the tumor to be easily defined.

More rapid clearance of blood-pool radioactivity was achieved with Fab fragments. The images obtained with

TABLE 2. TUMOR TO NONTUMOR RATIOS FOR ANTI-CEA AND MOPC21 AND THEIR FRAGMENTS

	Day 1*		Day 2		Day 3		Day 5	
	Anti-CEA	MOPC	Anti-CEA	MOPC	Anti-CEA	MOPC	Anti-CEA	MOPC
<b>Liver</b>								
Fab	2.8 (1.7-4.62)	1.9 (1.41-2.82) <sup>†</sup>	5.0 (3.35-9.28)	2.7 (1.66-4.67) <sup>‡</sup>	4.8 (2.63-6.26) <sup>†</sup>	2.6 (1.78-3.39) <sup>‡</sup>	2.4 (1.70-4.98) <sup>†</sup>	2.0 (1.50-2.39)
F(ab') <sub>2</sub>	5.2 (4.0-7.23) <sup>†</sup>	2.3 (1.59-3.34) <sup>‡</sup>	8.4 (5.39-10.21)	2.3 (2.22-3.68) <sup>‡</sup>	8.0 (7.57-8.54)	2.9 (2.69-3.38) <sup>‡</sup>	6.2 (5.65-6.76)	2.8 (2.61-3.01) <sup>‡</sup>
IgG	2.8 (2.04-3.35)	2.7 (2.08-3.25)	5.8 (5.25-6.30)	5.4 (4.33-5.76)	7.2 (5.56-8.85)	4.6 (4.06-4.83) <sup>‡</sup>	7.8 (6.38-9.82)	4.3 (3.97-3.01) <sup>‡</sup>
<b>Kidney</b>								
Fab	0.5 (0.30-0.82) <sup>†</sup>	0.1 (0.07-0.23) <sup>‡</sup>	1.0 (0.53-1.67)	0.3 (0.09-0.45) <sup>‡</sup>	1.2 (0.85-1.84)	0.6 (0.33-1.06) <sup>‡</sup>	0.7 (0.45-1.17)	0.6 (0.23-0.88)
F(ab') <sub>2</sub>	2.5 (1.69-3.66)	0.4 (0.33-0.56) <sup>‡</sup>	4.2 (3.02-5.92) <sup>†</sup>	0.4 (0.29-0.44) <sup>‡</sup>	6.2 (4.78-8.58)	0.6 (0.54-0.81) <sup>‡</sup>	4.7 (2.60-5.82) <sup>†</sup>	1.2 (0.69-1.37) <sup>‡</sup>
IgG	3.2 (1.92-4.40)	2.4 (1.60-3.16)	7.2 (6.56-7.88)	5.4 (4.73-5.90)	8.2 (5.50-10.53)	4.5 (3.94-6.09) <sup>‡</sup>	8.1 (7.53-9.24)	4.0 (3.44-4.62) <sup>‡</sup>
<b>Lung</b>								
Fab	1.4 (0.99-2.15) <sup>†</sup>	0.6 (0.26-0.81)	3.3 (2.10-4.74)	1.1 (0.66-1.96) <sup>‡</sup>	4.6 (2.05-7.49)	1.2 (0.65-1.65) <sup>‡</sup>	3.5 (1.98-5.47) <sup>†</sup>	1.2 (0.39-2.30) <sup>‡</sup>
F(ab') <sub>2</sub>	3.0 (2.64-3.21)	0.9 (0.91-0.93)	5.0 (2.87-7.31)	1.0 (0.71-1.57) <sup>‡</sup>	8.3 (6.52-10.41) <sup>†</sup>	1.6 (1.30-2.14) <sup>‡</sup>	6.2 (4.78-7.48)	2.0 (1.75-2.15) <sup>‡</sup>
IgG	2.3 (1.90-2.92)	1.7 (1.45-1.96)	4.2 (3.94-4.64)	3.1 (2.58-3.59)	5.2 (4.06-6.64)	2.8 (2.60-2.94) <sup>‡</sup>	5.7 (5.32-6.59)	2.7 (1.98-3.23) <sup>‡</sup>
<b>Spleen</b>								
Fab	2.5 (1.07-4.03)	0.9 (0.39-1.36) <sup>‡</sup>	8.6 (4.03-19.38)	1.3 (0.74-2.80) <sup>‡</sup>	7.0 (4.80-11.60)	1.8 (1.15-2.47) <sup>‡</sup>	2.6 (1.80-3.40)	1.8 (1.44-2.47) <sup>‡</sup>
F(ab') <sub>2</sub>	4.6 (3.37-6.50)	1.2 (0.70-1.63) <sup>‡</sup>	9.0 (5.37-11.87)	2.0 (1.05-3.82) <sup>‡</sup>	14.3 (11.16-17.68) <sup>†</sup>	2.3 (1.97-2.64) <sup>‡</sup>	6.7 (5.41-7.30) <sup>†</sup>	1.7 (1.64-1.82) <sup>‡</sup>
IgG	3.2 (2.90-3.73)	2.4 (2.10-2.56) <sup>‡</sup>	6.0 (5.71-6.12)	4.7 (4.01-5.55) <sup>‡</sup>	7.7 (6.51-10.38)	4.6 (4.12-5.51) <sup>‡</sup>	8.9 (6.89-10.60)	4.4 (3.85-4.67) <sup>‡</sup>
<b>Blood</b>								
Fab	0.8 (0.46-1.38)	0.5 (0.31-0.87) <sup>‡</sup>	1.7 (1.31-2.36)	0.7 (0.50-0.86) <sup>‡</sup>	2.0 (1.18-3.16)	0.7 (0.50-0.82) <sup>‡</sup>	1.5 (0.76-2.35)	0.5 (0.39-0.83) <sup>‡</sup>
F(ab') <sub>2</sub>	1.3 (0.97-1.74) <sup>†</sup>	0.4 (0.35-0.56) <sup>‡</sup>	2.4 (1.59-3.36)	0.6 (0.45-0.71) <sup>‡</sup>	2.8 (2.58-3.11) <sup>†</sup>	0.7 (0.66-0.86) <sup>‡</sup>	2.4 (1.92-2.75) <sup>†</sup>	0.9 (0.84-0.97) <sup>‡</sup>
IgG	0.7 (0.47-0.80)	0.5 (0.42-0.63)	1.4 (1.28-1.45)	1.0 (0.91-1.18) <sup>‡</sup>	1.8 (1.34-2.22)	1.0 (0.92-1.25) <sup>‡</sup>	1.9 (1.76-2.05)	1.0 (0.84-1.21) <sup>‡</sup>

\* Four animals injected with Fab anti-CEA and MOPC were sacrificed at 6 hr post-injection. Tumor/non-tumor ratios were: for anti-CEA, T/liver = 1.7, T/kidney, 0.12, T/lung, 0.56, T/spleen, 1.9, T/blood, 0.38; for MOPC, T/liver, 1.42, T/kidney, 0.08, T/lung, 0.43, T/spleen, 0.99, and T/blood, 0.27.

Sixty-two hamsters were injected as stated in the legend to Table 1. Ratios are cpm/g of anti-CEA or MOPC in the tumor divided by cpm/g in the stated tissue. Values are a mean and range for 3-8 animals. Corrections were made for downscatter for the <sup>131</sup>I channel.

<sup>†</sup> Statistically different from other anti-CEA moieties (p < 0.05).

<sup>‡</sup> Statistically different from mean for anti-CEA (p < 0.01).

**TABLE 3. ANTIBODY SPECIFIC LOCALIZATION RATIOS MEAN AND RANGE FOR INTACT AND F(ab')<sub>2</sub> AND FAB FRAGMENTS**

	Day 1*	Day 2	Day 3	Day 5
<b>Liver</b>				
Fab	1.5 (0.8–1.8)	2.0 (1.5–2.1)	1.8 (1.4–2.5)	1.2 (0.8–1.6)
†F(ab') <sub>2</sub>	2.3 (2.0–2.7)	3.1 (2.4–4.5)	2.8 (2.5–3.0)	2.2 (1.9–2.5)
IgG	1.0 (1.0–1.1)	1.1 (1.0–1.2)	1.6 (1.3–2.2)	1.8 (1.5–2.1)
<b>Kidney</b>				
Fab	5.1 (2.5–7.9)	5.4 (1.8–5.9)	2.3 (1.3–3.8)	1.6 (0.6–3.1)
F(ab') <sub>2</sub>	6.1 (5.1–6.5)	11.9 (8.5–19.1)	9.9 (8.4–10.6)†	3.6 (3.7–4.2)†
IgG	1.3 (1.2–1.4)†	1.3 (1.2–1.4)†	1.8 (1.4–2.5)	2.1 (1.8–2.2)
<b>Lung</b>				
Fab	2.7 (1.3–4.3)	3.6 (1.5–3.7)	3.7 (2.5–4.9)	3.6 (1.7–6.3)
F(ab') <sub>2</sub>	3.3 (2.9–3.5)	5.0 (3.8–8.2)	5.1 (4.6–5.4)	3.1 (2.7–3.6)
†IgG	1.3 (1.2–1.5)	1.4 (1.3–1.5)	1.8 (1.4–2.6)	2.2 (1.6–2.9)
<b>Spleen</b>				
Fab	3.7 (2.0–4.2)	7.4 (3.7–18.2)	3.8 (2.1–10.1)	2.9 (1.1–2.1)
F(ab') <sub>2</sub>	3.9 (2.9–4.8)	5.6 (2.2–9.7)	6.0 (5.0–7.5)	3.9 (2.3–4.3)
†IgG	1.4 (1.2–1.5)	1.3 (1.1–1.4)	1.7 (1.2–2.4)	2.0 (1.5–2.6)

\* Four animals were also sacrificed at 6 hr after injection with anti-CEA Fab-anti-MOPC Fab. Specific localization ratios: liver, 1.2; kidney, 1.5; lung, 1.3; spleen, 1.9; and blood, 1.4.

Sixty-two hamsters were injected as described in the legend to Table 1. Antibody specific localization ratios are calculated from anti-CEA tumor-to-nontumor ratios (Table 2) divided by MOPC21 tumor-to-nontumor ratios (Table 2). Means and ranges for 3–8 animals.

† Significantly different ( $p \leq 0.025$ ) from other means by regression analysis or student T-test.

Fab certainly reflect this faster clearance, with high levels of imaged radioactivity in the kidneys and bladder, the organs of excretion, as well as in the stomach on some images, in part due to consumption of I-131 laden litter. A rapid drop in whole-animal radioactivity made imaging with the 50  $\mu$ Ci dose impossible by 4 days. Due to the rapid clearance and the development of relatively high levels in the kidney at an early time point (6 hr), I-131-labeled Fab fragments in our judgment are not optimal agents for tumor imaging. Anti-CEA Fab at 6 hr showed 0.3% of the injected dose bound per gram and at 24 hr showed about 0.22% of injected dose binding to the tumor per gram. At 5 days this decreased to 0.018% binding per gram. This rapid tumor clearance parallels the fall in blood levels of Fab (Table 1) and has some precedent. Stelos et al. (27) showed in a rabbit anti-kidney model that fixation of Fab fragments was transitory relative to the more permanent fixation of intact Ab. Their data, however, showed that at 1 day Fab and intact Ab had comparable uptake in the target organ. Further studies with conclusive demonstration of the stability of the radiolabeled antibody fragment will be needed to confirm our impression that this is actually lower binding due possibly to univalency of the binding site and not due in large measure to deiodination, though both phenomena may be contributory.

Images obtained with F(ab')<sub>2</sub> delineated the tumor earlier and with less background radioactivity than intact

Ab at comparable time points. Our subjective opinion was that the 3–4 day F(ab')<sub>2</sub> images overall were better than 11-day intact-antibody images since less background radioactivity was present. Better definition was particularly apparent in the 4–5 g tumors on injection but was also true for the 1–2 g tumors. There is no question that the localization is specific as evidenced by the anti-CEA compared with MOPC control images (Figs. 4–6).

Of note is the fact that the F(ab')<sub>2</sub> radioactivity fades from the tumor faster than that of the intact Ab. This is in excess of the physical decay expected. At 24 hr after injection approximately 1.77% of the injected dose of anti-CEA F(ab')<sub>2</sub> was bound to the tumor per g, but by 5 days this dropped to approximately 0.3%, after correction for physical decay. For intact Ab there was a drop as well from 2.6% of injected dose bound/g at 2 days to approximately 1.5% at 5 days. During this period, tumor clearance of intact antibody and fragments closely paralleled the blood clearance, and suggests that the decline in tumor concentrations was mainly dependent upon an equilibrium between antibody or fragment and the circulating Ab or fragments in the blood. Some of this fall in tumor levels also may have been due to shedding of CEA with bound anti-CEA or conceivably to in vivo deiodination. This relatively lower accretion of F(ab')<sub>2</sub> in the tumor as a percentage of injected dose was apparently still relatively greater because of the still lower



accretion of  $F(ab')_2$  in the other organs, particularly the blood. It may be necessary to use larger doses of  $F(ab')_2$  for tumor imaging than intact Ab to detect small foci due to the fast clearance of  $F(ab')_2$  relative to intact Ab. Even with an increase in dose, the radiation exposure to the patient could still be less than intact Ab with  $F(ab')_2$  due to its faster clearance.

This gradual loss from the tumor of intact antibody and  $F(ab')_2$  radioactivity is undesirable if long-term delivery of radiation to a tumor by antibody is planned. It is possible, however, that this shorter residence time of  $F(ab')_2$  at the tumor might be overridden by repeated administration in therapy. In any case, it does not preclude imaging. This phenomenon for  $F(ab')_2$  seems akin to that described by Stelos et al. for Fab (27). Other investigators, however, have shown that the binding of  $F(ab')_2$  to antigen is quite stable (28).

The double-label experiment supported the imaging data with the  $F(ab')_2$  fragment of anti-CEA showing the best tumor localization with tumor-to-blood ratios at 2 days for  $F(ab')_2$  significantly better ( $p < 0.025$ ) than those for intact anti-CEA or Fab fragments. This superiority of  $F(ab')_2$  anti-CEA tumor-to-blood ratios was seen for all time points in the study. In addition, this tumor localization was more specific than the accretion of comparable MOPC  $F(ab')_2$  fragments. The tumor-to-tissue ratios showed generally good tumor localization of all three forms of anti-CEA, but comparison with matching MOPC ratios was most striking for  $F(ab')_2$ . Intact anti-CEA and MOPC showed little difference in tumor-to-blood ratios until 3 to 5 days after injection, when further clearance of MOPC had occurred and nonspecific binding was less prevalent. This gradual attainment of significant differences in tumor-to-nontumor ratios for intact antibody, compared with MOPC is likely due in part to nonspecific binding of the Fc fragment. The specific binding for intact antibody eventually dominated but not until 3–5 days after injection. For the fragments the anti-CEA developed a significant difference from MOPC by 1–2 days after injection. Their lack of the Fc may well have allowed the earlier specific localization to occur.

The fact that higher specific localization ratios exist for  $F(ab')_2$  in the liver, lung, and spleen where large populations of Fc receptor positive cells reside than exist for intact Ab supports the concept that Fc elimination may be largely responsible for this improved specific localization. These data show that satisfactory radioimmunodetection of tumors in this system can occur with and without simple background subtraction much faster with  $F(ab')_2$  than with intact Ab. In addition, significantly higher ratios of specific localization and tissue-to-blood ratios were present with the use of  $F(ab')_2$  than with intact Ab or Fab. In addition, absolute tumor-to-tissue ratios were higher for  $F(ab')_2$  than for intact Ab in the blood, spleen, liver and lung at several

early time points. These are all desirable qualities for imaging. The high level of specific binding of anti-CEA  $F(ab')_2$  relative to MOPC  $F(ab')_2$  conceivably could be exploited in future background subtraction systems, using the simultaneously administered nonspecific antibody fragment as the subtracting agent. The marked difference between specific and nonspecific  $F(ab')_2$  would then be tumor-specific. This development awaits appropriate improvements in labeling and further experiments. Also of importance is the possibility that by the use of higher and more frequently repeated injected doses, more  $F(ab')_2$  will specifically accumulate in tumors with a higher therapeutic ratio than intact antibody. Based on these findings, we believe that  $F(ab')_2$  fragments will assume an increasingly important role in immunodiagnostic systems in vivo by decreasing the need for background subtraction, allowing earlier imaging, potentially serving as better background subtraction agents, and possibly in immunotherapy as vehicles of toxin or radionuclide delivery. Further work is needed in these areas.

#### FOOTNOTES

\* Adapted Hoffman-LaRoche CEA kit.

† Abbott Laboratories, Chicago, IL.

#### ACKNOWLEDGMENTS

The authors thank Dr. David Goldenberg for the GW-39 tumor, Dr. R. Fulton for the MOPC21 ascites, Dr. C. Lockhart, Dr. H. W. Margraf, and M. Bauman for help in producing and characterizing the monoclonal anti-CEA, S. Wahl and K. Hopkins for expert technical assistance, and J. Havranek for editorial help with the manuscript.

Support from The Jewish Hospital of St. Louis and NCI Grant CA 16217 is appreciated.

#### REFERENCES

1. PRESSMAN D, KORNGOLD L: The in vivo localization of anti-Wagner-osteogenic-sarcoma antibodies. *Cancer* 6: 619–623, 1953
2. CHAO H, PEIPER SC, PHILPOTT GW, et al: Selective uptake of specifically purified antibodies to carcinoembryonic antigen of human adenocarcinoma. *Research Communications in Chemical Pathology and Pharmacology* 9:749–761, 1974
3. GOLDENBERG DM, DELAND FH, KIM EE, et al: Use of radiolabelled antibodies to a carcinoembryonic antigen for the detection and localization of diverse cancers by external photoscanning. *N Engl J Med* 298:1384–1388, 1978
4. MACH J-P, CARREL S, FORNI M, et al: Tumor localization of radiolabeled antibodies against carcinoembryonic antigen in patients with carcinoma. A Critical Evaluation. *N Engl J Med* 303:5–10, 1980
5. BALLOU B, LEVINE G, HAKALA T, et al: Tumor location detected with radioactively labeled monoclonal antibody and external scintigraphy. *Science* 206:844–847, 1979
6. MACH JP, BUCHEGGER F, FORNI M, et al: Use of radiolabelled monoclonal anti-CEA antibodies for the detection of human carcinoma by external photoscanning and tomoscintigraphy. *Immunol Today* 2:239–249, 1981

7. SPIEGELBERG HL, WEIGLE WO: The catabolism of homologous and heterologous 7s gamma globulin fragments. *J Exp Med* 121:323-338, 1965
8. WAHL R, PHILPOTT G, PARKER C: Monoclonal antibody radioimmunoassay of human-derived colon cancer. *Invest Radiol* (in press)
9. HOFFER PB, LATHROP K, BEKERMANN C, et al: Use of <sup>131</sup>I-CEA antibody as a tumor scanning agent. *J Nucl Med* 15:323-327, 1974
10. PRIMUS FJ, WANG RM, GOLDENBERG DM, et al: Localization of human GW-39 tumors in hamsters by radiolabeled heterospecific antibody to carcinoembryonic antigen. *Cancer Res* 33:2977-2983, 1973
11. BEIHN RM, DAMVON JR, HAFNER T: Subtraction technique for the detection of subphrenic abscesses using <sup>67</sup>Ga and <sup>99m</sup>Tc. *J Nucl Med* 15:371-373, 1974
12. DELAND FH, KIM E, SIMMONS G, et al: Imaging approach in radioimmunoassay. *Cancer Res* 40:3046-3049, 1980
13. HOPF U, ZUM BÜSCHENFELDE KHM, DIERICH MP: Demonstration of binding sites for IgG Fc and the third complement component (C 3) on isolated hepatocytes. *J Immunol* 117:639-645, 1976
14. KHAW BA, BELLER GA, HABER E, et al: Localization of cardiac myosin-specific antibody in myocardial infarction. *J Clin Invest* 58, 439-446, 1976
15. KOJI T, ISHII N, MUNEHISA T, et al: Localization of radioiodinated antibody to alpha-fetoprotein in rats with transplanted hepatocellular carcinoma. *Oncodev Biol Med* 1:359-368, 1980
16. MACH JP, FORNI M, RITSCHARD J, et al: Use and limitations of radiolabeled anti-CEA antibodies and their fragments for photoscanning detection of human colorectal carcinomas. *Oncodev Biol Med* 1:49-69, 1980
17. BURCHIEL SW, KHAW BA, RHODES BA, et al: Immunopharmacokinetics of radiolabeled antibodies and their fragments. In *Tumor Imaging*. Burchiel, SW and Rhodes BA, Eds. Masson Publishing, New York, 1982, pp 125-140
18. GAFFAR SA, BENNETT SJ, DELAND FH, et al: Carcinoembryonic antigen (CEA) radioactive antibody fragment for cancer localization in vivo. *Proc Am Assoc Cancer Res* 23:249
19. GOLDENBERG DM, WITTE S, ELSTER K: GW-39: A new human tumor serially transplantable in the Golden hamster. *Transplantation* 4:760-763, 1966
20. LOCKHART CG, STINSON RS, MARGRAF HW, et al: Production of anti-carcinoembryonic antigen (CEA) antibody by somatic cell hybridization. *Fed Proc* 39:3476, 1980
21. GALFRÉ G, HOWE SC, MILSTEIN C, et al: Antibodies to major histocompatibility antigens produced by hybrid cell lines. *Nature* 266:550-552, 1977
22. PHILPOTT GW, GRASS EH, PARKER CW: Affinity cytotoxicity with an alcohol dehydrogenase-antibody conjugate and allyl alcohol. *Cancer Res* 39:2084-2089, 1979
23. MISHILL B, SHIIGI S, Eds: *Selected Methods in Cellular Immunology*, Chicago, W. H. Freeman, 1980, pp 284-285
24. NISONOFF A, MARKUS G, WISSLER FC, et al: Separation of univalent fragments of rabbit antibody by reduction of disulfide bonds. *Arch Biochem* 89:230-244, 1960
25. LAEMMLI UK: Cleavage of structural proteins during the assembly of the head of bacteriophage T4. *Nature* 227: 680-685, 1970
26. PRESSMAN D, DAY ED, BLAU M: The use of paired labeling in the determination of tumor-localizing antibodies. *Cancer Res* 17:845-850, 1957
27. STELOS P, YAGI Y, PRESSMAN D: Localization properties of radioiodinated fragments of antirrat kidney antibody. *J Immunol* 87:106-109, 1961
28. MASRI M, BOYD N, ALEXANDER F, et al: Irreversible attachment of immunoglobulins and F(ab')<sub>2</sub> fragments to their specific cell membrane antigens. *Transplantation* 30:373-376, 1980

## International Symposium on Single-Photon Ultra-Short-Lived Radionuclides

**May 9-10, 1983**

**PAHO**

**Washington, DC**

The Society of Nuclear Medicine, the American College of Nuclear Physicians, the Department of Energy and Department of Radiological Health are sponsoring the International Symposium on Single-Photon Ultra-Short-Lived Radionuclides on May 9-10, 1983 at PAHO in Washington, DC.

The objective of this symposium is to define the current role and state of the art of development and clinical applications of generator-produced single-photon ultra-short-lived radionuclides (USRN).

This symposium will emphasize the phases of generator production, quality control, dosimetry, instrumentation, and clinical applications of USRN. Principal focus will be on the Ir-191m, Au-185m and Br-81m radionuclide generators. The sessions are designed to encourage active participation and discussion.

Scientific presentations 12 minutes in length pertinent to objectives of the program are being solicited. Submit 1 page abstracts with supporting data to the ACNP with a registration form. Deadline for abstracts is February 15th. The program committee will arrange with authors for specifics of presentation.

Manuscripts of at least 3 pages long are due on arrival at the symposium; Proceedings will be published by the Department of Energy and DRH.

For further information contact:

Erica Kellison  
American College of Nuclear Physicians  
Suite 700  
1101 Connecticut Avenue  
Washington, DC 20036